SOLUTION OF THE NAVIER-STOKES EQUATIONS IN THREE-DIMENSIONS USING THE JAMESON AND MAVRIPLIS ALGORITHM - PART II

Edisson Sávio de Góes Maciel
Rua Demócrito Cavalcanti, 152 - Afogados
Recife – PE – Brazil - CEP 50750-080
e-mail: edissonsavio@yahoo.com.br

Abstract. This work presents the Jameson and Mavriplis algorithm applied to the solution of the Navier-Stokes equations in three-dimensions, solving aerospace problems. A finite volume formulation is used, with a cell centered data base and using a structured spatial discretization. The scheme is second order accurate in space and time. The time integration uses a Runge-Kutta method of five stages. An artificial dissipation operator based on Azevedo work is implemented to guarantee numerical stability in the presence of shock waves and background instability. A spatially variable time step is implemented aiming to accelerate the convergence process to steady state solution. The physical problems of the supersonic flow along a ramp and of the "cold gas" hypersonic flow along a diffuser are solved. In the ramp problem the shock is well detected and in the diffuser problem the shock interference is well solved. A final analysis of the computational performance (maximum CFL number and iterations to convergence) is accomplished.

Keywords: Jameson and Mavriplis algorithm, Navier-Stokes equations, Finite volumes, Three-dimensions, Supersonic and hypersonic flows.

1. Introduction

It is necessary to solve the Navier-Stokes equations in three-dimensions using turbulence models more precise to obtain more realistic flow properties, inside a reasonable cost interval. Direct simulations or large eddy simulation are still very expensive and require a high computational power which is still elevated to Brazil. Three-dimension studies start with inviscid simulations, aiming to check the solver to typical problems, and, posteriorly, are intensified to the solution of the laminar Navier-Stokes equations and finally to the turbulent Navier-Stokes equations.

Pulliam and Steger (1980) performed studies with the Navier-Stokes equations, in its thin layer formulation, applied to three-dimension flows. An implicit finite difference scheme was used for unsteady flow simulations in configurations of arbitrary geometry through the use of a generalized coordinate system. An implicit approximated factorization technique was employed aiming to obtain better stability conditions in the solution of the viscous flows. The authors emphasized that the implemented scheme could be used to inviscid and viscous, unsteady and steady flows.

Long, Khan and Sharp (1991) developed a method to the solution of the Euler and the Navier-Stokes equations in the three-dimensions. The method was developed in a finite volume formulation and the spatial discretization could be structured or unstructured to hexahedral or tetrahedral meshes, respectively. It was used a cell centered data structure and the time integration was performed by a Runge-Kutta method of three, four or five stages. The scheme could be symmetrical, with an artificial dissipation operator to guarantee numerical stability, or upwind. In the upwind case, it was used the Roe (1981) scheme. Tests were accomplished with Delta and Lockheed/AFOSR wings.

In the present work, the Jameson and Mavriplis (1986) scheme is implemented, on the finite volume context and using a structured spatial discretization, to solve the Navier-Stokes equations in three-dimensions applied to the problems of the supersonic flow along a ramp and the "cold gas" hypersonic flow along a diffuser. The implemented scheme is second order accurate in space and time. It is necessary the introduction of a dissipation operator to guarantee stability to the scheme and the Azevedo (1992) model is implemented. The algorithm is accelerated to steady state solution using a spatially variable time step. The results have demonstrated that the Jameson and Mavriplis (1986) scheme supplies satisfactory solutions, detecting the main flow characteristics. It is important to emphasizes that this is not the first time that the Jameson and Mavriplis (1986) scheme is implemented in its version to three-dimensions (Long, Khan and Sharp, 1991, for example) but it is objective of study of the present author.

2. Navier-Stokes equations

The fluid movement is described by the Navier-Stokes equations, which express the conservation of mass, of momentum and of energy to a viscous, heat conductor and compressible mean, in the absence of external forces. In the integral and conservative forms, these equations can be represented by:

$$\partial/\partial t \int_V Q dV + \int_S \left[(E_e - E_v)n_x + (F_e - F_v)n_y + (G_e - G_v)n_z \right] dS = 0, \tag{1}$$

where Q is written to a Cartesian system; V is the cell volume; n_x, n_y and n_z are normal unity vector components to the flux face; S is the flux area; E_e, F_e and G_e are the convective flux vector components; and E_v, F_v and G_v are the diffusive

flux vector components. The vectors Q, E_e, F_e, G_e, E_v, F_v and G_v are represented by:

$$Q = \begin{Bmatrix} \rho \\ \rho u \\ \rho v \\ \rho w \\ e \end{Bmatrix}, \quad E_e = \begin{Bmatrix} \rho u \\ \rho u^2 + p \\ \rho uv \\ \rho uw \\ (e+p)u \end{Bmatrix}, \quad F_e = \begin{Bmatrix} \rho v \\ \rho uv \\ \rho v^2 + p \\ \rho vw \\ (e+p)v \end{Bmatrix} \quad \text{and} \quad G_e = \begin{Bmatrix} \rho w \\ \rho uw \\ \rho vw \\ \rho w^2 + p \\ (e+p)w \end{Bmatrix}; \tag{2}$$

$$E_v = \frac{1}{Re} \begin{Bmatrix} 0 \\ \tau_{xx} \\ \tau_{xy} \\ \tau_{xz} \\ \tau_{xx}u + \tau_{xy}v + \tau_{xz}w - q_x \end{Bmatrix}, \quad F_v = \frac{1}{Re} \begin{Bmatrix} 0 \\ \tau_{yx} \\ \tau_{yy} \\ \tau_{yz} \\ \tau_{yx}u + \tau_{yy}v + \tau_{yz}w - q_y \end{Bmatrix} \quad \text{and} \quad G_v = \frac{1}{Re} \begin{Bmatrix} 0 \\ \tau_{zx} \\ \tau_{zy} \\ \tau_{zz} \\ \tau_{zx}u + \tau_{zy}v + \tau_{zz}w - q_z \end{Bmatrix}. \tag{3}$$

In these equations, the components of the viscous stress tensor are defined as:

$$\tau_{xx} = 2\mu \frac{\partial u}{\partial x} - \frac{2}{3}\mu \left(\frac{\partial u}{\partial x} + \frac{\partial v}{\partial y} + \frac{\partial w}{\partial z} \right), \quad \tau_{xy} = \mu \left(\frac{\partial u}{\partial y} + \frac{\partial v}{\partial x} \right), \quad \tau_{xz} = \mu \left(\frac{\partial u}{\partial z} + \frac{\partial w}{\partial x} \right),$$

$$\tau_{yy} = 2\mu \frac{\partial v}{\partial y} - \frac{2}{3}\mu \left(\frac{\partial u}{\partial x} + \frac{\partial v}{\partial y} + \frac{\partial w}{\partial z} \right), \quad \tau_{zz} = 2\mu \frac{\partial w}{\partial z} - \frac{2}{3}\mu \left(\frac{\partial u}{\partial x} + \frac{\partial v}{\partial y} + \frac{\partial w}{\partial z} \right) \quad \text{and} \quad \tau_{yz} = \mu \left(\frac{\partial v}{\partial z} + \frac{\partial w}{\partial y} \right). \tag{4}$$

The components of the conducted heat flux vector are defined by the Fourier law as follows:

$$q_x = -\left(\frac{\gamma\mu}{Pr} \right) \frac{\partial e_i}{\partial x}, \quad q_y = -\left(\frac{\gamma\mu}{Pr} \right) \frac{\partial e_i}{\partial y} \quad \text{and} \quad q_z = -\left(\frac{\gamma\mu}{Pr} \right) \frac{\partial e_i}{\partial z}, \tag{5}$$

where ρ is the fluid density; u, v and w are the Cartesian components of the velocity vector in the x, y and z directions, respectively; e is the total energy per unity volume; p is the static pressure; μ represents the fluid molecular viscosity; Prd is the laminar Prandtl number; γ is the ratio of specific heats; Re is the flow Reynolds number; and e_i is the fluid internal energy, defined as

$$e_i = e/\rho - 0.5\left(u^2 + v^2 + w^2 \right). \tag{6}$$

The Navier-Stokes equations were nondimensionalized in relation to the freestream density, ρ_∞, the freestream speed of sound, a_∞, and the freestream molecular viscosity, μ_∞, for the studied problems. The matrix system of the Navier-Stokes equations is closed with the state equation of a perfect gas:

$$p = (\gamma - 1)\left[e - 0.5\rho(u^2 + v^2 + w^2) \right]. \tag{7}$$

3. Jameson and Mavriplis (1986) algorithm

Using the Green theorem in Equation (1) and adopting a structured mesh notation to the fluid properties and of the flow, it is possible to write that:

$$\partial Q_{i,j,k} / \partial t = -1/V_{i,j,k} \int_{S_{i,j,k}} (\vec{P} \cdot \vec{n})_{i,j,k} \, dS_{i,j,k}, \tag{8}$$

with $\vec{P} = \begin{bmatrix} E_e & F_e & G_e \end{bmatrix}^t$, being the convective flux vector. A given computational cell in this notation is formed by the following nodes: *(i,j,k)*, *(i+1,j,k)*, *(i+1,j+1,k)*, *(i,j+1,k)*, *(i,j,k+1)*, *(i+1,j,k+1)*, *(i+1,j+1,k+1)* and *(i,j+1,k+1)*. Details of this representation are available in Maciel (2002) and in Maciel (2004). The calculation of the computational cell volumes is based, in the more general case, on the determination of the volume of one deformed hexahedral in three-dimensions. This volume is determined by the sum of the volumes of the six tetrahedral which comprise the given hexahedral. The division of the hexahedral in its six tetrahedral components, as well as the vertex nodes which define

each cell, can be found in details in Maciel (2002) and in Maciel (2004). In Maciel (2002) is also found details of the calculation of a given tetrahedral volume.

The hexahedral flux area is calculated by the sum of the half areas defined by the norm of the external products $|\vec{a} \, x \, \vec{b}|$ and $|\vec{c} \, x \, \vec{d}|$, where $\vec{a}$, $\vec{b}$, $\vec{c}$ and $\vec{d}$ are vectors formed by the nodes which define a given flux surface, as described in Maciel (2002) and in Maciel (2004). The physical quantity $0.5(|\vec{a} \, x \, \vec{b}| + |\vec{c} \, x \, \vec{d}|)$ determines the flux area of each face, which is the area of a deformed rectangle. The normal unity vectors to each flux face are calculated considering the external product $\vec{r} \, x \, \vec{t} / |\vec{r} \, x \, \vec{t}|$ where $\vec{r}$ and $\vec{t}$ are surface crossed vectors (they are the surface diagonals). An additional test is necessary aiming to verify if the normal unity vector is inward or outward of the hexahedral. This test is based on the scalar product $[(\vec{r} \, x \, \vec{t}) \bullet \vec{f} / |\vec{r} \, x \, \vec{t}|]$, where $\vec{f}$ is the vector formed by two nodes: one node refer to the flux face and the other node refer to the immediately opposite face. The positive signal indicates that the vector is inward in the hexahedral. In this case, the vector should be changed by its opposite.

The Equation (8) can be rewritten as follows:

$$d(Q_{i,j,k})/dt + 1/V_{i,j,k} \left[(\vec{P} \cdot \vec{S})_{i,j-1/2,k} + (\vec{P} \cdot \vec{S})_{i+1/2,j,k} + (\vec{P} \cdot \vec{S})_{i,j+1/2,k} + (\vec{P} \cdot \vec{S})_{i-1/2,j,k} + \right.$$
$$\left. (\vec{P} \cdot \vec{S})_{i,j,k-1/2} + (\vec{P} \cdot \vec{S})_{i,j,k+1/2} \right]^n = 0 \ , \tag{9}$$

with:

$$(\vec{P} \cdot \vec{S})_{i,j-1/2,k} = \left[(E_e)_{i,j-1/2,k} S_{x_{i,j-1/2,k}} + (F_e)_{i,j-1/2,k} S_{y_{i,j-1/2,k}} + (G_e)_{i,j-1/2,k} S_{z_{i,j-1/2,k}} \right] \tag{10}$$

representing the interface flux *(i,j-1/2,k)*, for example. The inviscid flux vectors in each flux interface are implemented considering the arithmetical average of the primitive variables in each face; in other words, to the flux face *(i,j-1/2,k)* is possible to determine the primitive variables at interface using arithmetical average between values of the primitive variable of the volumes *(i,j-1,k)* and *(i,j,k)*:

$$\rho_{i,j-1/2,k} = 0.5(\rho_{i,j-1,k} + \rho_{i,j,k}), \quad u_{i,j-1/2,k} = 0.5(u_{i,j-1,k} + u_{i,j,k}), \quad v_{i,j-1/2,k} = 0.5(v_{i,j-1,k} + v_{i,j,k}),$$
$$w_{i,j-1/2,k} = 0.5(w_{i,j-1,k} + w_{i,j,k}) \quad \text{and} \quad e_{i,j-1/2,k} = 0.5(e_{i,j-1,k} + e_{i,j,k}). \tag{11}$$

The spatial discretization proposed by the authors is symmetrical on the context of a finite difference technique. With the purpose of avoiding uncoupled solutions, nonlinear instabilities (shock waves), etc., it is explicitly introduced an artificial dissipation operator "D" to provide scheme numerical stability. In the present code was implemented the artificial dissipation model based on Azevedo (1992) work. So, Equation (9) can be rewritten as:

$$d(Q_{i,j,k})/dt + 1/V_{i,j,k} \left[C(Q_{i,j,k}) - D(Q_{i,j,k}) \right] = 0 , \tag{12}$$

where:

$$C(Q_{i,j,k}) = \left[(\vec{P} \cdot \vec{S})_{i,j-1/2,k} + (\vec{P} \cdot \vec{S})_{i+1/2,j,k} + (\vec{P} \cdot \vec{S})_{i,j+1/2,k} + (\vec{P} \cdot \vec{S})_{i-1/2,j,k} + (\vec{P} \cdot \vec{S})_{i,j,k-1/2} + (\vec{P} \cdot \vec{S})_{i,j,k+1/2} \right]^n \tag{13}$$

is the flux integral to the cell *(i,j,k)*.

The time integration is performed using a hybrid explicit Runge-Kutta method with first or second order of accuracy. The more general form of this method is presented bellow, where the values of the α coefficients are chosen to provide first or second order of time accuracy, as well as to invest certain properties to the scheme which benefit the use of the "multigrid" convergence acceleration technique.

$$Q_{i,j,k}^{(0)} = Q_{i,j,k}^n \ ,$$
$$Q_{i,j,k}^{(l)} = Q_{i,j,k}^{(0)} - \alpha_l \, \Delta t_{i,j,k} / V_{i,j,k} \left[C(Q_{i,j,k}^{(l-1)}) - D(Q_{i,j,k}^{(m)}) \right] \ , \tag{14}$$
$$Q_{i,j,k}^{n+1} = Q_{i,j,k}^{(l)} \ .$$

where "*l*" varies from 1 to 5; "*m*" varies according to the type of the studied flow (inviscid or viscous). Swanson and Radespiel (1991) suggests that the artificial dissipation should be evaluated in alternate stages when the Navier -Stokes

equations were solved (*m* = 1, 3 and 5, in the five stage case). This procedure aims to allow a CPU time economy and also better smooth the numerical instabilities of the discretization based on the parabolic/hyperbolic characteristics of the Navier-Stokes equations.

The Runge-Kutta method with one stage is reduced to the explicit Euler method, first order accurate. The value of α in this case is 1.0. The Runge-Kutta method of two stages and more, until five stages, is second order accurate in time and the values of α are defined bellow:

a) Two stages: $\alpha_1 = 1/2$ and $\alpha_2 = 1.0$;
b) Three stages: $\alpha_1 = 1/2$, $\alpha_2 = 1/2$ and $\alpha_3 = 1.0$;
c) Four stages: $\alpha_1 = 1/4$, $\alpha_2 = 1/3$, $\alpha_3 = 1/2$ and $\alpha_4 = 1.0$;
d) Five stages: $\alpha_1 = 1/4$, $\alpha_2 = 1/6$, $\alpha_3 = 3/8$, $\alpha_4 = 1/2$ and $\alpha_5 = 1.0$.

To the calculation of the viscous flux vectors, the derivatives present in Eqs. (4) and (5) are considered constants to a given volume and calculated in terms of the property surface integral along the control volume faces (Green theorem):

$$\frac{\partial u}{\partial x} = \frac{1}{V} \int_V \frac{\partial u}{\partial x} dV = \frac{1}{V} \int_S u(\vec{n}_x \bullet d\vec{S}) = \frac{1}{V} \int_{S_x} u dS_x \cong \frac{1}{V} \sum_{l=1}^{6} u_{i,j,k_l} S_{x\,i,j,k_l} \quad , \tag{15}$$

$$\frac{\partial v}{\partial y} = \frac{1}{V} \int_V \frac{\partial v}{\partial y} dV = \frac{1}{V} \int_S v(\vec{n}_y \bullet d\vec{S}) \cong \frac{1}{V} \int_{S_y} v dS_y \cong \frac{1}{V} \sum_{l=1}^{6} v_{i,j,k_l} S_{y\,i,j,k_l} \quad , \tag{16}$$

$$\frac{\partial w}{\partial z} = \frac{1}{V} \int_V \frac{\partial w}{\partial z} dV = \frac{1}{V} \int_S w(\vec{n}_z \bullet d\vec{S}) = \frac{1}{V} \int_{S_z} w dS_z \cong \frac{1}{V} \sum_{l=1}^{6} w_{i,j,k_l} S_{z\,i,j,k_l} \quad , \tag{17}$$

where, for example, u_{i,j,k_l} is the arithmetical average between cell (i,j,k) and its respective neighbor. The value of the derivative $\partial u/\partial x$ at flux interface *(i,j-1/2,k)*, for example, is determined by the arithmetical average of the derivatives $\partial u/\partial x$ of volumes *(i,j,k)* and *(i,j-1,k)*.

3.1. Artificial dissipation operator

The artificial dissipation operator implemented in the Jameson and Mavriplis (1986) code to simulate three-dimension flows follows the structure bellow:

$$D(Q_{i,j,k}) = d^{(2)}(Q_{i,j,k}) - d^{(4)}(Q_{i,j,k}) \quad , \tag{18}$$

where:

$$
\begin{aligned}
d^{(2)}(Q_{i,j,k}) = {} & \varepsilon_{i,j,k,1}^{(2)} \frac{(A_{i,j,k} + A_{i,j-1,k})}{2}(Q_{i,j-1,k} - Q_{i,j,k}) + \varepsilon_{i,j,k,2}^{(2)} \frac{(A_{i,j,k} + A_{i+1,j,k})}{2}(Q_{i+1,j,k} - Q_{i,j,k}) \\
& + \varepsilon_{i,j,k,3}^{(2)} \frac{(A_{i,j,k} + A_{i,j+1,k})}{2}(Q_{i,j+1,k} - Q_{i,j,k}) + \varepsilon_{i,j,k,4}^{(2)} \frac{(A_{i,j,k} + A_{i-1,j,k})}{2}(Q_{i-1,j,k} - Q_{i,j,k}) \\
& + \varepsilon_{i,j,k,5}^{(2)} \frac{(A_{i,j,k} + A_{i,j,k-1})}{2}(Q_{i,j,k-1} - Q_{i,j,k}) + \varepsilon_{i,j,k,6}^{(2)} \frac{(A_{i,j,k} + A_{i,j,k+1})}{2}(Q_{i,j,k+1} - Q_{i,j,k}),
\end{aligned}
\tag{19}
$$

named undivided Laplacian operator, is responsible to the numerical stability in the presence of shock waves;

$$
\begin{aligned}
d^{(4)}(Q_{i,j,k}) = {} & \varepsilon_{i,j,k,1}^{(4)} \frac{(A_{i,j,k} + A_{i,j-1,k})}{2}(\nabla^2 Q_{i,j-1,k} - \nabla^2 Q_{i,j,k}) + \varepsilon_{i,j,k,2}^{(4)} \frac{(A_{i,j,k} + A_{i+1,j,k})}{2}(\nabla^2 Q_{i+1,j,k} - \nabla^2 Q_{i,j,k}) \\
& + \varepsilon_{i,j,k,3}^{(4)} \frac{(A_{i,j,k} + A_{i,j+1,k})}{2}(\nabla^2 Q_{i,j+1,k} - \nabla^2 Q_{i,j,k}) + \varepsilon_{i,j,k,4}^{(4)} \frac{(A_{i,j,k} + A_{i-1,j,k})}{2}(\nabla^2 Q_{i-1,j,k} - \nabla^2 Q_{i,j,k}) \\
& + \varepsilon_{i,j,k,5}^{(4)} \frac{(A_{i,j,k} + A_{i,j,k-1})}{2}(\nabla^2 Q_{i,j,k-1} - \nabla^2 Q_{i,j,k}) + \varepsilon_{i,j,k,6}^{(4)} \frac{(A_{i,j,k} + A_{i,j,k+1})}{2}(\nabla^2 Q_{i,j,k+1} - \nabla^2 Q_{i,j,k}),
\end{aligned}
\tag{20}
$$

named biharmonic operator, is responsible by the background stability. The following term

$$\nabla^2 Q_{i,j,k} = [(Q_{i,j-1,k} - Q_{i,j,k}) + (Q_{i+1,j,k} - Q_{i,j,k}) + (Q_{i,j+1,k} - Q_{i,j,k}) + (Q_{i-1,j,k} - Q_{i,j,k}) + (Q_{i,j,k-1} - Q_{i,j,k}) + (Q_{i,j,k+1} - Q_{i,j,k})] \tag{21}$$

is named Laplacian of $Q_{i,j,k}$. In the operator $d^{(4)}$, $\nabla^2 Q_{i,j,k}$ is extrapolated from its real neighbor every time that it represents a special boundary cell, recognized in the literature as "ghost" cell. The ε terms are defined as follows:

$$\varepsilon_{i,j,k,1}^{(2)} = K^{(2)} MAX\left(\nu_{i,j,k}, \nu_{i,j-1,k}\right), \ \varepsilon_{i,j,k,2}^{(2)} = K^{(2)} MAX\left(\nu_{i,j,k}, \nu_{i+1,j,k}\right), \ \varepsilon_{i,j,k,3}^{(2)} = K^{(2)} MAX\left(\nu_{i,j,k}, \nu_{i,j+1,k}\right),$$

$$\varepsilon_{i,j,k,4}^{(2)} = K^{(2)} MAX\left(\nu_{i,j,k}, \nu_{i-1,j,k}\right), \ \varepsilon_{i,j,k,5}^{(2)} = K^{(2)} MAX\left(\nu_{i,j,k}, \nu_{i,j,k-1}\right) \text{ and } \varepsilon_{i,j,k,6}^{(2)} = K^{(2)} MAX\left(\nu_{i,j,k}, \nu_{i,j,k+1}\right);$$

$$(22)$$

$$\varepsilon_{i,j,k,1}^{(4)} = MAX\left[0, \left(K^{(4)} - \varepsilon_{i,j,k,1}^{(2)}\right)\right], \ \varepsilon_{i,j,k,2}^{(4)} = MAX\left[0, \left(K^{(4)} - \varepsilon_{i,j,k,2}^{(2)}\right)\right], \ \varepsilon_{i,j,k,3}^{(4)} = MAX\left[0, \left(K^{(4)} - \varepsilon_{i,j,k,3}^{(2)}\right)\right],$$

$$\varepsilon_{i,j,k,4}^{(4)} = MAX\left[0, \left(K^{(4)} - \varepsilon_{i,j,k,4}^{(2)}\right)\right], \ \varepsilon_{i,j,k,5}^{(4)} = MAX\left[0, \left(K^{(4)} - \varepsilon_{i,j,k,5}^{(2)}\right)\right] \text{ and } \varepsilon_{i,j,k,6}^{(4)} = MAX\left[0, \left(K^{(4)} - \varepsilon_{i,j,k,6}^{(2)}\right)\right], \quad (23)$$

where:

$$\nu_{i,j,k} = \frac{\left|p_{i+1,j,k} - p_{i,j,k}\right| + \left|p_{i,j+1,k} - p_{i,j,k}\right| + \left|p_{i-1,j,k} - p_{i,j,k}\right| + \left|p_{i,j,k-1} - p_{i,j,k}\right| + \left|p_{i,j-1,k} - p_{i,j,k}\right| + \left|p_{i,j,k+1} - p_{i,j,k}\right|}{p_{i,j-1,k} + p_{i+1,j,k} + p_{i,j+1,k} + p_{i-1,j,k} + p_{i,j,k-1} + p_{i,j,k+1} + 6\,p_{i,j,k}} \quad (24)$$

represents a pressure sensor, responsible by the identification of regions of high gradients. The constants $K^{(2)}$ and $K^{(4)}$ has typical values of 1/4 and 3/256, respectively. Every time that a neighbor represents a ghost cell, it is assumed that, for example, $\nu_{i,j-1,k} = \nu_{i,j,k}$. The $A_{i,j,k}$ coefficient was implemented as proposed by Azevedo (1992) and is defined as:

$$A_{i,j,k} = V_{i,j,k} / \Delta t_{i,j,k} \ . \tag{25}$$

4. Spatially variable time step

The idea of a spatially variable time step consists in keeping constant a CFL number in the calculation domain and to guarantee time steps appropriated to each mesh region during the convergence process. Details of the present implementation can be found in Maciel (2002) and in Maciel (2004).

5. Initial and boundary conditions

5.1. Initial condition

The initial condition adopted to the problems is the freestream flow in all calculation domain (Jameson and Mavriplis, 1986, Maciel, 2002, and Maciel, 2004).

5.2. Boundary conditions

The different types of implemented boundary conditions are described as follows.
a)   Wall - To the Navier-Stokes case, the velocity components u, v and w of the ghost volumes are equaled to the respective values of u, v and w of the neighbor real volume, with opposite signal.

$$u_g = -u_{real} \ , \ v_g = -v_{real} \text{ and } w_g = -w_{real} \ . \tag{26}$$

The fluid pressure gradient in the direction normal to the wall is equal to zero for the viscous case. The temperature gradient is equal to zero along all wall, with this last situation according to the physical results, without impose, however, the condition of adiabatic wall. With these two conditions, a zero order extrapolation is performed to the pressure and to the temperature. It is also concluded that the fluid density is obtained by zero order extrapolation.
b)   Far field - In the implementation of the boundary conditions in the mesh limit external region to physical problems of external flow, it is necessary to identify four possible situations: entrance with subsonic flow, entrance with supersonic flow, exit with subsonic flow and exit with supersonic flow. These situations are described bellow.
b.1) Entrance with subsonic flow – Considering the one-dimensional characteristic relation concept in the normal direction of flow penetration, the entrance with subsonic flow presents four characteristic velocities of information propagation which have direction and orientation point inward the calculation domain, which implies that the variables associated with these waves can not be extrapolated (Maciel and Azevedo, 1997, Maciel and Azevedo, 1998b, Maciel, 2002, and Maciel, 2004). It is necessary to specify four conditions to these four information. Jameson and Mavriplis (1986) indicate as appropriated quantities to be specified the freestream density and the freestream Cartesian velocity components u, v and w. Just the last characteristics, "(q_n-a)", which transports information from inside to outside of the calculation domain, can not be specified and will have to be determined by interior information of the calculation domain. In this work, a zero order extrapolation to the pressure is performed, being the total energy defined by the state

equation of a perfect gas.

b.2) Entrance with supersonic flow - All variables are specified in the entrance boundary, adopting freestream values.

b.3) Exit with subsonic flow - Four characteristics which govern the Euler equations proceed from the internal region of the calculation domain. So, the density and the Cartesian velocity components are extrapolated from the interior domain. One condition should be specified to the boundary. In this case, the pressure is fixed in the calculation domain exit, keeping its respective value of freestream flow.

b.4) Exit with supersonic flow - The five characteristics which govern the Euler equations proceed from the internal region of the calculation domain. It is not possible to specify variable values at the exit. The zero order extrapolation is applied to density, Cartesian velocity components and pressure.

c) Entrance and exit – The entrance and exit boundaries are applied to both problems. Boundary conditions which involve flow entrance in the calculation domain had the flow properties fixed with freestream values. Boundary conditions which involve flow exit of the computational domain used simply the zero order extrapolation to the determination of properties in this boundary. This procedure is correct because the entrance flow and the exit flow are no minimal supersonic to both studied examples.

6. Results

Tests were accomplished in an ATHLON-2.6GHz and 64 Mbytes of RAM memory microcomputer. Converged results occurred to 4 orders of reduction in the maximum residual value. The value used to γ was 1.4. The configuration downstream and the configuration longitudinal plane angles were set equal to 0.0°.

6.1. Ramp physical problem

The algebraic mesh has 42,660 real volumes and 48,800 nodes to the structured discretization of the calculation domain. It is equivalent to a mesh with 61 points in the ξ direction, 80 points in the η direction and 10 points in the ς direction. To this problem, ramp with 20º of inclination, it was adopted a freestream Mach number of 5.0 as initial condition. It was considered a flight altitude of 30,000 meters and the ramp characteristic length assumed the value 0.044 meter. With the altitude is possible to determine values of freestream density, freestream pressure and freestream viscosity and is possible to calculate the Reynolds number of this simulation, which was 403,143.7.
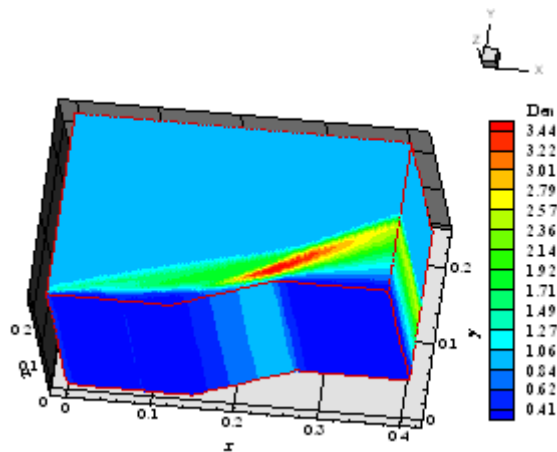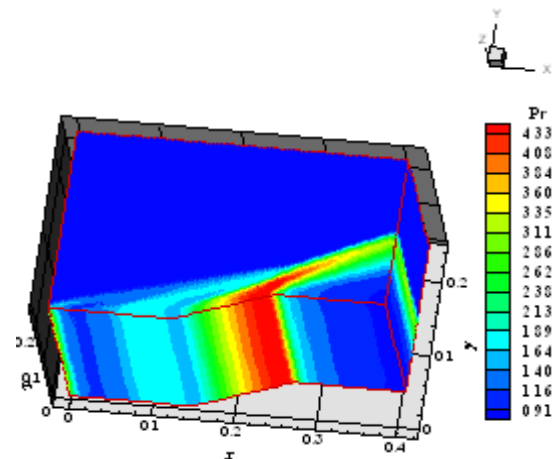

Figure 1 – Density field.
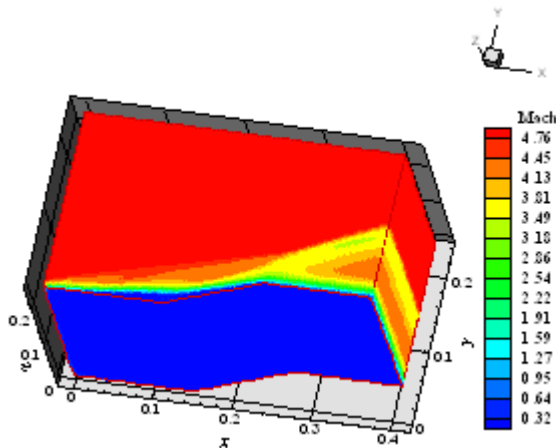

Figure 2 – Pressure field.
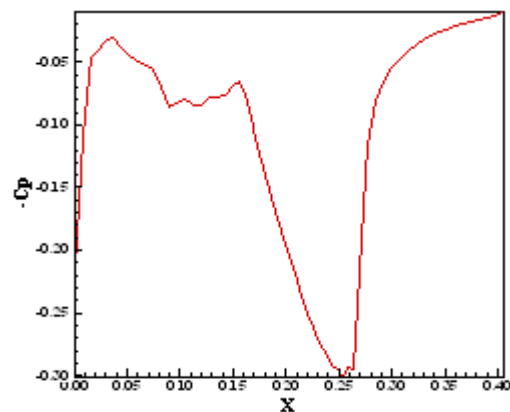

Figure 3. Mach number field.

Figure 4. -Cp distribution.

Figures 1, 2 and 3 present the density, the pressure and the Mach number contours, respectively, obtained by the Jameson and Mavriplis (1986) scheme to this problem. Figure 3 is free of pre-shock oscillations. The shock is well detected in the pressure and density contours. The solution is repeated in all planes "k", which is the expected behavior.

Figure 4 presents the –Cp distribution along the ramp obtained by the Jameson and Mavriplis (1986) scheme, in the section k = kmax/2, where "kmax" is the maximum number of points in the z direction. As can be observed, the shock wave is not adequately represented but the expansion fan is appropriated described. The CFL number used by the scheme was 0.8 and the convergence has occurred in 3,011 iterations. The computational cost of the Jameson and Mavriplis (1986) algorithm is 0.0002538s/per volume/per iteration. It is important to note that this cost is constant to every inviscid simulation with this algorithm, independent of the studied physical problem.

6.2. Diffuser physical problem

In this case, the mesh has 32,400 real volumes and 37,210 nodes to the structured discretization of the calculation domain. It is equivalent to a mesh of 61 points in the ξ direction, 61 points in the η direction and 10 points in the ς direction. The initial condition to this problem of the "cold gas" hypersonic flow along a diffuser with 20º of inclination adopted a value of the freestream Mach number equals to 10.0, flight altitude of 40,000 meters. The diffuser characteristic length was 0.21 meter and the Reynolds number of this simulation was calculated in 166,312.48.
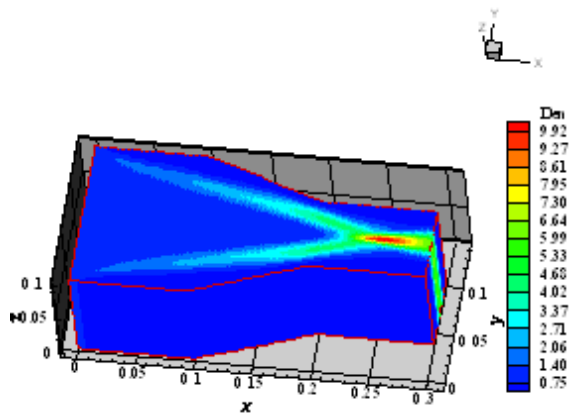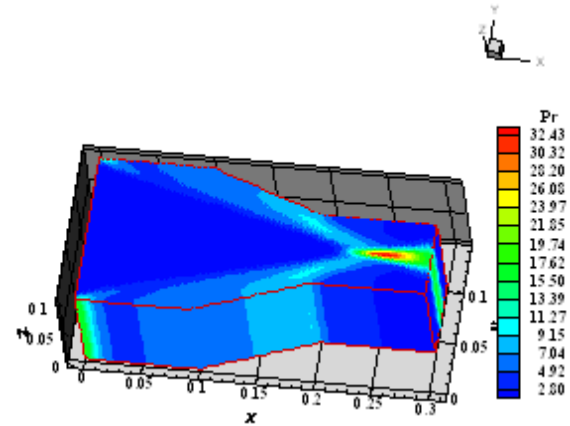

Figure 5. Density field.

Figure 6. Pressure field.

Figures 5, 6 and 7 present the density, the pressure and the Mach number contours, respectively, obtained by the Jameson and Mavriplis (1986) scheme. The density and pressure contours present good symmetry and the shock interference is well detected. The Mach number contours are free of pre-shock oscillations.

Figure 8 shows the –Cp distribution along the diffuser lower wall, in the section k = kmax/2. The shock and the expansion fan are not correctly described. The CFL number used in this simulation was 0.2 and the convergence to steady state solution occurred in 9,245 iterations.
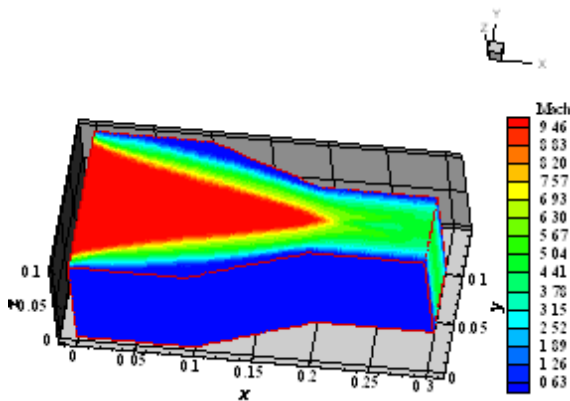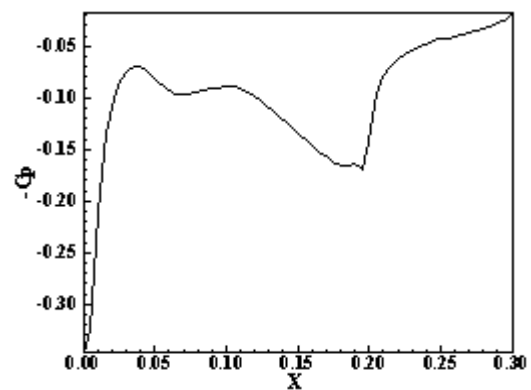

Figure 7. Mach number field.

Figure 8. -Cp distribution.

7. Conclusions

This work presented the Jameson and Mavriplis (1986) scheme implemented in its version to three-dimensions. The algorithm is explicit, second order accurate in space and time and integrated in time by a Runge-Kutta method of five stages. The Navier-Stokes equations were solved, using a finite volume formulation, with a cell centered data base and

structured discretization. The physical problems of the supersonic flow along a ramp and the "cold gas" hypersonic flow along a diffuser were solved. A spatially variable time step was implemented aiming to accelerate the convergence process to steady state condition.

The results obtained were of good quality, without occur pre-shock oscillations in the Mach number contours. The density and the pressure fields presented good behavior highlighting well the shock in the ramp problem and detecting appropriately the shock interference in the diffuser problem. The -Cp distributions do not show well the shock and the expansion fan in both problems. The computational cost of the present implementation of the Jameson and Mavriplis (1986) algorithm is 0.0002538s/per volume/per iteration.

8. Acknowledgements

9. References

Azevedo, J. L. F., 1992, "On the Development of Unstructured Grid Finite Volume Solvers for High Speed Flows", NT-075-ASE-N, IAE, CTA, São José dos Campos, SP.

Jameson, A. and Mavriplis, D., 1986, "Finite Volume Solution of the Two-Dimensional Euler Equations on a Regular Triangular Mesh", AIAA Journal, Vol. 24, No. 4, pp. 611-618.

Long, L. N, Khan, M. M. S., and Sharp, H. T., 1991, "Massively Parallel Three-Dimensional Euler / Navier-Stokes Method", AIAA Journal, Vol. 29, No. 3, pp. 657-666.

Maciel, E. S. G. and Azevedo, J. L. F., 1997, "Comparação entre Vários Algoritmos de Fatoração Aproximada na Solução das Equações de Navier-Stokes", Proceedings of the 14th Brazilian Congress of Mechanical Engineering (available in CD-ROM), Bauru, SP, Brazil.

Maciel, E. S. G. and Azevedo, J. L. F., 1998, "Comparação entre Vários Esquemas Implícitos de Fatoração Aproximada na Solução das Equações de Navier-Stokes", RBCM- Journal of the Brazilian Society of Mechanical Sciences, Vol. XX, No. 3, pp. 353-380.

Maciel, E. S. G., 2002, "Simulação Numérica de Escoamentos Supersônicos e Hipersônicos Utilizando Técnicas de Dinâmica dos Fluidos Computacional", Doctoral thesis, ITA, CTA, São José dos Campos, SP, Brazil, 258 p.

Maciel, E. S. G., 2004, "Relatório ao Conselho Nacional de Pesquisa e Desenvolvimento Tecnológico (CNPq) sobre as Atividades de Pesquisa Desenvolvidas no Primeiro Ano de Vigência da Bolsa de Estudos para Nível DCR-IF Referente ao Processo nº 304318/2003-5", Technical repport to CNPq, November, 37 p.

Pulliam, T. H., and Steger, J. L., 1980, "Implicit Finite-Difference Simulations of three-Dimensional Compressible Flow", AIAA Journal, Vol. 18, No. 2, pp. 159-166.

Roe, P. L., 1981, "Approximate Riemann Solvers, Parameter Vectors, and Difference Schemes", Journal of Computational Physics, Vol. 43, pp. 357-372.

Swanson, R. C. and Radespiel, R., 1991, "Cell Centered and Cell Vertex Multigrid Schemes for the Navier-Stokes Equations", AIAA Journal, Vol. 29, No. 5, pp. 697-703.

10. Responsibility notice